We are IntechOpen, the world's leading publisher of Open Access books Built by scientists, for scientists

4,800
Open access books available

122,000
International authors and editors

135M
Downloads

Our authors are among the

154
Countries delivered to

TOP 1%
most cited scientists

12.2%
Contributors from top 500 universities

CLARIVATE ANALYTICS BOOK CITATION INDEX INDEXED

WEB OF SCIENCE™

Selection of our books indexed in the Book Citation Index in Web of Science™ Core Collection (BKCI)

Interested in publishing with us?
Contact book.department@intechopen.com

Numbers displayed above are based on latest data collected.
For more information visit www.intechopen.com

6

Global Stiffness Optimization of Parallel Robots Using Kinetostatic Performance Indices

Dan Zhang
University of Ontario Institute of Technology
Canada

1. Introduction

Global Stiffness design and optimization of parallel mechanisms can be a difficult and time-consuming exercise in parallel robot design, especially when the variables are multifarious and the objective functions are too complex. To address this issue, optimization techniques based on kinetostatic model and genetic algorithms are investigated as the effective criteria. First, a 5-DOF parallel mechanism with a passive constraining leg and five identical legs with prismatic actuators for machine tool is proposed, and its corresponding inverse kinematics, Jacobian matrices and global velocity equation are derived. Second, with the kinetostatic model, the mean value and the standard deviation of the trace of the global compliance distribution are proposed as these two kinetostatic performance indices. Finally, the effectiveness of this optimization design methodology for global stiffness indices is validated with simulation.

Compared with traditional serial manipulators, a parallel robot manipulator offers different potential benefits, including high rigidity, high accuracy, and high loading capacities. The parallel robot manipulator is used for applications where the demand on workspace and manoeuvrability is relatively low, while the dynamic loading is severe, and high speed and precision motions are primarily required. These applications include parallel kinematic machines (PKMs), aircraft flight simulators, telescope positioning, position tracker, and medical devices (Zhang & Gosselin, 2000; Dunlop & Jones, 1999; Carretero & Podhorodeski, 2000; Staicu *et al*., 2006; Zhang & Wang, 2000; Liu *et al*., 2005). Past research and development efforts with parallel robot manipulators have shown the ever-increasing demand on the robot's rigidity which is directly related to the system stiffness. In order to increase the production, a parallel manipulator which is capable of high speed operations with optimal rigidity is necessary.

Recently, researchers have been trying to utilize these advantages to develop parallel robot based multi-axis machining tools and precision assembly tools. Since most machining operations only require a maximum of five axes, new configurations with less than six axes would be more appropriate (Bi *et al*., 2005). A 5-DOF parallel mechanism with a passive constraining leg and five identical legs with prismatic actuators for machine tool is proposed in this work. Kinetostatic analysis is essential for PKMs. A great deal of work so far has been

done on kinetostatic analysis that has direct application to PKMs (Birglen & Gosselin, 2004; Chablat & Angeles, 2002; Zhang & Gosselin, 2002), the issue of how to optimize the global stiffness based on kinetostatic modelling has not been well addressed. Two global compliance indices (kinetostatic performance indices) are introduced in this study, namely, the mean value and the standard deviation of the trace of the generalized stiffness matrix. The mean value represents the average stiffness of the PKMs over the workspace, while the standard deviation indicates the stiffness fluctuation relative to the mean value.

Many scholars have studied on optimum design of robot manipulators (Bergamaschi *et al*, 2006; Stock & Miller, 2003; Rout & Mittal, 2008; Ceccarelli & Lanni, 2004). Lum *et al.* (Mitchell *et al*., 2006) presented kinematic optimization to confirm the smallest configuration that would satisfy the workspace requirements for a lightweight and compact surgical manipulator. Chablat and Angeles (Chablat & Angeles, 2002) investigated on optimum dimensioning of revolute-coupled planar manipulators based on the concept of distance of Jacobian matrix to a given isotropic matrix which was used as a reference model. Zhao *et al.* (Zhao *et al*., 2007) exploited the least number method of variables to optimize the leg length of a spatial parallel manipulator. Boeij *et al.* (Boeij *et al*., 2008) proposed numerical integration and sequential quadratic programming method for optimization of a contactless electromagnetic planar 6-DOF actuator with manipulator on top of the floating platform. However, the traditional optimization methods only handle a few geometric variables due to the lack of convergence of the optimization algorithm. Genetic algorithms have applied the powerful and broadly applicable stochastic search methods and optimization techniques, and they can escape from local optima (Holland, 1975).

The remainder of the chapter is organized as follows. In Section 2, the structure of the tripod parallel manipulator and its parametric description is introduced. In Section 3, the kinetostatic analysis and stiffness modelling process is derived. In Section 4, the application of the integration approach is conducted to optimize the performance indices. Finally, the conclusions are given in Section 5.

2. Structure of the parallel manipulator

In this work, a 5-DOF parallel mechanism and its joint distributions both on the base and on the platform are shown in Figures 1, 2. This mechanism consists of six kinematic chains, including five variable length legs with identical topology and one passive leg which connect the fixed base to the moving platform. In this 5-DOF parallel mechanism, the kinematic chains associated with the five identical legs consist, from base to platform, of a fixed Hooke joint, a moving link, an actuated prismatic joint, a second moving link and a spherical joint attached to the platform. The sixth chain (central leg) connecting the base centre to the platform is a passive constraining leg and has architecture different from the other chains. It consists of a revolute joint attached to the base, a moving link, a Hooke joint, a second moving link and another Hooke joint attached to the platform. This last leg is used to constrain the motion of the platform to only five degrees of freedom. This mechanism could be built using only five legs, i.e., by removing one of the five identical legs and actuating the first joint of the passive constraining leg. However, the uniformity of the actuation would be lost.

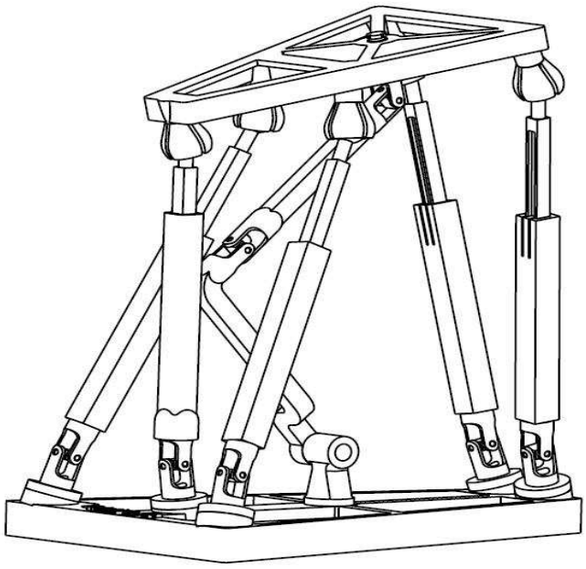

Fig. 1. CAD model of the 5-DOF parallel manipulator (by Gabriel Cote)

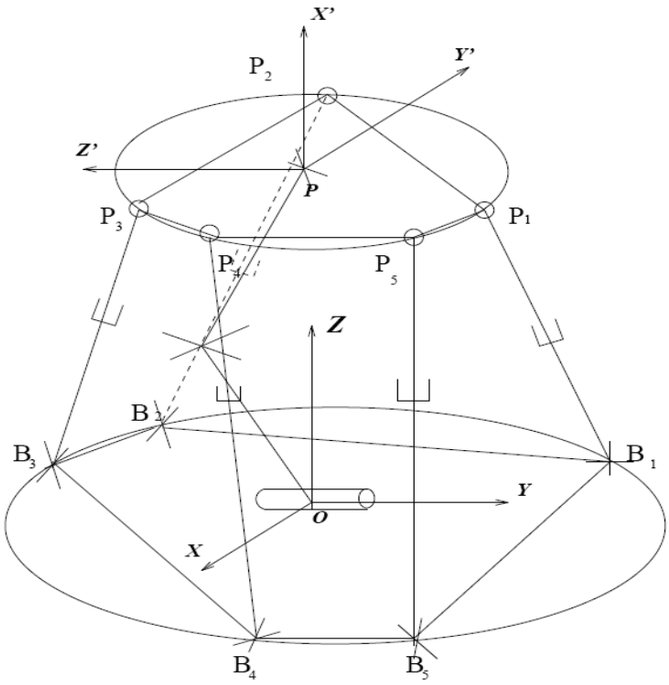

Fig. 2. Schematic representation of the 5-DOF parallel mechanism

Assume that the centres of the joints located on the base and on the platform are located on circles with radii $\mathbf{R_b}$ and $\mathbf{R_p}$, respectively. A fixed reference frame **O-xyz** is attached to the base of the mechanism and a moving coordinate frame **P-x′y′z′** is attached to the platform. In Figure 2, the points of attachment of the actuated legs to the base are represented with $\mathbf{B_i}$

and the points of attachment of all legs to the platform are represented by $\mathbf{P_i}$, with i=1...5. Point **P** is the reference point on the platform and its position coordinate is **P(x,y,z).**
The Cartesian coordinates of the platform are given by the position of point **P** with respect to the fixed frame, and the orientation of the platform (orientation of frame **P – x′y′z′** with respect to the fixed frame), represented by rotation matrix **Q**.
If the coordinates of the point $\mathbf{P_i}$ in the moving reference frame are represented with ($\mathbf{x_i'}$,$\mathbf{y_i'}$,$\mathbf{z_i'}$) and the coordinates of the point B_i in the fixed frame are represented by vector $\mathbf{b_i}$, then for i=1,...,5, one has

$$\mathbf{p}_i = \left[x_i, y_i, z_i\right]^T \tag{1}$$

$$\mathbf{r}_i' = \left[x_i', y_i', z_i'\right]^T \tag{2}$$

$$\mathbf{p} = \left[x, y, z\right]^T \tag{3}$$

$$\mathbf{b}_\mathrm{i} = \left[b_{ix}, b_{iy}, b_{iz}\right]^T \tag{4}$$

Where $\mathbf{P_i}$ is the position vector of point $\mathbf{P_i}$ expressed in the fixed coordinate frame whose coordinates are defined as ($\mathbf{x_i}$,$\mathbf{y_i}$,$\mathbf{z_i}$), $\mathbf{r_i'}$ is the position vector of point $\mathbf{P_i}$ expressed in the moving coordinate frame, and **P** is the position vector of point **P** expressed in the fixed frame as defined above.
One can then write

$$\mathbf{p}_\mathrm{i} = \mathbf{p} + \mathbf{Q}\mathbf{r}_i', \ i = 1,\ldots,5 \tag{5}$$

Where, **Q** is the rotation matrix from the fixed reference frame to the moving coordinate frame.
Subtracting vector $\mathbf{b_i}$ from both sides of Eq. (5), one obtains

$$\mathbf{p}_\mathrm{i} - \mathbf{b}_\mathrm{i} = \mathbf{p} + \mathbf{Q}\mathbf{r}_\mathrm{i}' - \mathbf{b}_i, \ i = 1,\ldots,5 \tag{6}$$

Then, taking the Euclidean norm on both sides of Eq. (6), one has

$$\left\|\mathbf{p}_\mathrm{i} - \mathbf{b}_\mathrm{i}\right\| = \left\|\mathbf{p} + \mathbf{Q}\mathbf{r}_\mathrm{i}' - \mathbf{b}_\mathrm{i}\right\| = \boldsymbol{\rho}_\mathrm{i}, \ i = 1,\ldots,5 \tag{7}$$

Where $\boldsymbol{\rho}_\mathbf{i}$ is the length of the ith leg, i.e., the value of the ith joint coordinate. The solution of the inverse kinematic problem for the 5-DOF manipulator is therefore completed and can be written as

$$\boldsymbol{\rho}_\mathrm{i}^2 = (\mathbf{p}_\mathrm{i} - \mathbf{b}_\mathrm{i})^\mathrm{T}(\mathbf{p}_\mathrm{i} - \mathbf{b}_\mathrm{i}), \ i = 1,\ldots,5 \tag{8}$$

Now considering the parallel component of the mechanism, the parallel Jacobian matrix can be obtained by differentiating Eq. (8) with respect to time, one obtains

$$\boldsymbol{\rho}_\mathrm{i}\dot{\boldsymbol{\rho}}_\mathrm{i} = (\mathbf{p}_\mathrm{i} - \mathbf{b}_\mathrm{i})^\mathrm{T}\dot{\mathbf{p}}_\mathrm{i}, \quad i = 1,\ldots,5 \tag{9}$$

Since one has

$$\dot{\boldsymbol{Q}} = \boldsymbol{\Omega Q} \tag{10}$$

with

$$\boldsymbol{\Omega} = 1 \times \boldsymbol{\omega} = \begin{bmatrix} 0 & -\omega_3 & \omega_2 \\ \omega_3 & 0 & -\omega_1 \\ -\omega_2 & \omega_1 & 0 \end{bmatrix} \tag{11}$$

differentiating Eq. (5), one obtains

$$\dot{\boldsymbol{p}}_i = \dot{\boldsymbol{p}} + \dot{\boldsymbol{Q}}\boldsymbol{r}_i' \tag{12}$$

Then, Eq. (9) can be rewritten as

$$\boldsymbol{\rho}_i \dot{\boldsymbol{\rho}}_i = (\mathbf{p}_i - \mathbf{b}_i)^{\mathrm{T}} \dot{\mathbf{p}} + [(\mathbf{Q}\mathbf{r}_i') \times (\mathbf{p}_i - \mathbf{b}_i)]^{\mathrm{T}} \boldsymbol{\omega}, \; i = 1, \ldots, 5 \tag{13}$$

Hence, one can write the velocity equation as

$$\mathbf{A}\boldsymbol{t} = \mathbf{B}\dot{\boldsymbol{\rho}} \tag{14}$$

where vector $\dot{\boldsymbol{\rho}}$ is defined as

$$\dot{\boldsymbol{\rho}} = \begin{bmatrix} \dot{\boldsymbol{\rho}}_1 & \dot{\boldsymbol{\rho}}_2 & \ldots\ldots & \dot{\boldsymbol{\rho}}_5 \end{bmatrix}^T \tag{15}$$

and

$$\mathbf{A} = [\mathbf{m}_1 \quad \mathbf{m}_2 \quad \cdots \quad \mathbf{m}_5]^T \tag{16}$$

$$\mathbf{B} = diag[\boldsymbol{\rho}_1 \quad \boldsymbol{\rho}_2 \quad \cdots \quad \boldsymbol{\rho}_5] \tag{17}$$

where $\mathbf{m}_i$ is a vector with 6 components, which can be expressed as

$$\mathbf{m}_i = \begin{bmatrix} (\mathbf{Q}\mathbf{r}_i') \times (\mathbf{p}_i - \mathbf{b}_i) \\ (\mathbf{p}_i - \mathbf{b}_i) \end{bmatrix} \tag{18}$$

3. Kinetostatic analysis and stiffness modelling

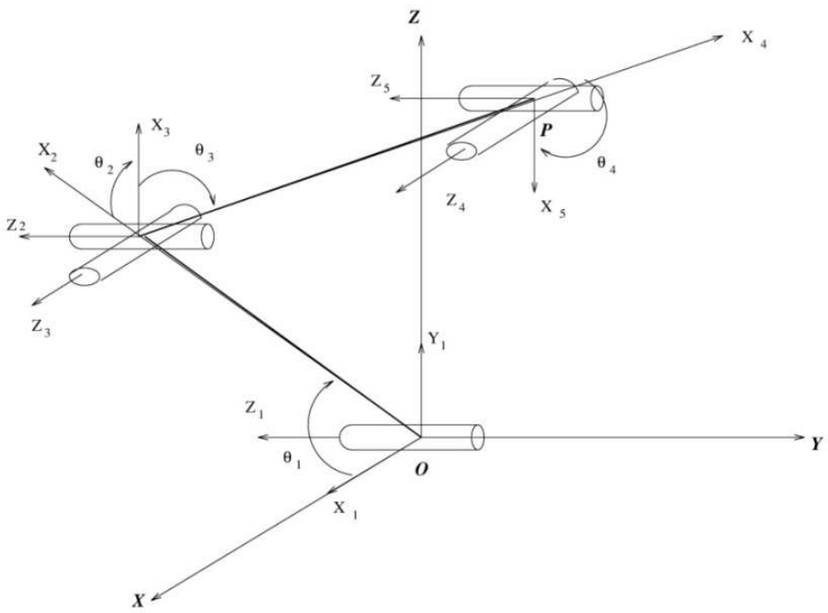

Fig. 3. The passive constraining leg with rigid links

i	a_i	b_i	α_i	θ_i
0	0	0	90°	0
1	$l_{passive,1}$	0	0	$\theta_{passive,1}$
2	0	0	90°	$\theta_{passive,2}$
3	$l_{passive,2}$	0	0	$\theta_{passive,3}$
4	0	0	90°	$\theta_{passive,4}$
5	0	0	0	$\theta_{passive,5}$

Table 1. The DH parameters for the passive constraining leg with rigid links

From Figure 3, one can obtain the Danavit-Hartenberg parameters of the passive leg as in Table 1. We take the Cartesian coordinate frame O, and define α_0=90°, θ_0=0°, then one obtains

$$\mathbf{Q}_{passive,0} = \begin{bmatrix} 1 & 0 & 0 \\ 0 & 0 & -1 \\ 0 & 1 & 0 \end{bmatrix} \tag{19}$$

The expressions for vectors $e_{passive,i}$ and $r_{passive,i}$ are then obtained following the procedure given above.

Stiffness is a very important factor in many applications including machine tool design, as it affects the precision of machining. Induced vibration is explicitly linked to machine tool stiffness. For a metal cutting machine tool, high stiffness allows higher machining speeds and feeds while providing the desired precision, thus reduce vibration (such as chatter). Therefore, to build and study a general stiffness model of parallel mechanisms is very important for machine tool design.

The parallel mechanisms studied here comprise two main components, namely, the constraining leg - which can be considered as a serial mechanism - and the actuated legs acting in parallel.

Considering the constraining leg, one can write

$$\mathbf{J}_{\text{passive}}\dot{\boldsymbol{\theta}}_{\text{passive}} = \mathbf{t} \tag{20}$$

where $\mathbf{t} = \begin{bmatrix} \boldsymbol{\omega}^T & \dot{\boldsymbol{p}}^T \end{bmatrix}^T$ is the twist of the platform, with $\boldsymbol{\omega}$ the angular velocity of the platform and

$$\dot{\boldsymbol{\theta}}_{\text{passive}} = \begin{bmatrix} \dot{\boldsymbol{\theta}}_{\text{passive},1} & \cdots & \dot{\boldsymbol{\theta}}_{\text{passive},5} \end{bmatrix}^T \tag{21}$$

$$\mathbf{J}_{\text{passive}} = \begin{bmatrix} \mathbf{e}_{\text{passive},1} & \mathbf{e}_{\text{passive},2} & \mathbf{e}_{\text{passive},3} & \mathbf{e}_{\text{passive},4} & \mathbf{e}_{\text{passive},5} \\ \mathbf{e}_{\text{passive},1} \times \mathbf{r}_{\text{passive},1} & \mathbf{e}_{\text{passive},2} \times \mathbf{r}_{\text{passive},2} & \mathbf{e}_{\text{passive},3} \times \mathbf{r}_{\text{passive},3} & \mathbf{e}_{\text{passive},4} \times \mathbf{r}_{\text{passive},4} & \mathbf{e}_{\text{passive},5} \times \mathbf{r}_{\text{passive},5} \end{bmatrix} \tag{22}$$

is the joint velocity vector associated with the constraining leg. Matrix $\mathbf{J}_{\text{passive}}$ is the Jacobian matrix of the constraining leg considered as a serial 5-dof mechanism.

According to the principle of virtual work, one has

$$\boldsymbol{\tau}^{\mathrm{T}}\dot{\boldsymbol{\rho}} = \mathbf{w}^{\mathrm{T}}\mathbf{t} \tag{23}$$

Where $\boldsymbol{\tau}$ is the vector of actuator forces applied at each actuated joint and $\mathbf{w}$ is the wrench (torque and force) applied to the platform and where it is assumed that no gravitational forces act on any of the intermediate links. In practice, gravitational forces may often be neglected in machine tool applications.

One has $\mathbf{w} = \begin{bmatrix} \mathbf{n}^T & \mathbf{f}^T \end{bmatrix}^T$ where $\mathbf{n}$ and $\mathbf{f}$ are respectively the external torque and force applied to the platform.

Rearranging Eq. (14) and substituting it into Eq. (23), one obtains

$$\boldsymbol{\tau}^{\mathrm{T}}\mathbf{B}^{-1}\mathbf{A}\mathbf{t} = \mathbf{w}^{\mathrm{T}}\mathbf{t} \tag{24}$$

Now, substituting Eq. (20) into Eq. (24), one has

$$\boldsymbol{\tau}^{\mathrm{T}}\mathbf{B}^{-1}\mathbf{A}\mathbf{J}_{\text{passive}}\dot{\boldsymbol{\theta}}_{\text{passive}} = \mathbf{w}^{\mathrm{T}}\mathbf{J}_{\text{passive}}\dot{\boldsymbol{\theta}}_{\text{passive}} \tag{25}$$

The latter equation must be satisfied for arbitrary values of $\dot{\boldsymbol{\theta}}_{\text{passive}}$ and hence one can write

$$(\mathbf{A}\mathbf{J}_{\text{passive}})^{\text{T}}\mathbf{B}^{-\text{T}}\boldsymbol{\tau} = \mathbf{J}_{\text{passive}}^{\text{T}}\mathbf{w} \tag{26}$$

The latter equation relates the actuator forces to the Cartesian wrench, w, applied at the end-effector in static mode. Since all links are assumed rigid, the compliance of the mechanism will be induced solely by the compliance of the actuators. An actuator compliance matrix C is therefore defined as

$$\mathbf{C}\boldsymbol{\tau} = \Delta\boldsymbol{\rho} \tag{27}$$

Where $\boldsymbol{\tau}$ is the vector of actuated joint forces and $\Delta\boldsymbol{\rho}$ is the induced joint displacement. Matrix **C** is a (n×n) diagonal matrix whose ith diagonal entry is the compliance of the **i**th actuator.
Now, Eq. (26) can be rewritten as

$$\boldsymbol{\tau} = \mathbf{B}^{\text{T}}(\mathbf{A}\mathbf{J}_{\text{passive}})^{-\text{T}}\mathbf{J}_{\text{passive}}^{\text{T}}\mathbf{w} \tag{28}$$

The substitution of Eq. (28) into Eq. (27) then leads to

$$\Delta\boldsymbol{\rho} = \mathbf{C}\mathbf{B}^{\text{T}}(\mathbf{A}\mathbf{J}_{\text{passive}})^{-\text{T}}\mathbf{J}_{\text{passive}}^{\text{T}}\mathbf{w} \tag{29}$$

Moreover, for a small displacement vector $\Delta\boldsymbol{\rho}$, Eq. (14) can be written as

$$\Delta\boldsymbol{\rho} \cong \mathbf{B}^{-1}\mathbf{A}\Delta\mathbf{c} \tag{30}$$

where $\Delta\mathbf{C}$ is a vector of small Cartesian displacement and rotation defined as

$$\Delta\mathbf{c} = \begin{bmatrix} \Delta\mathbf{p}^{\text{T}} & \Delta\boldsymbol{\alpha}^{\text{T}} \end{bmatrix}^{\text{T}} \tag{31}$$

in which $\Delta\boldsymbol{\alpha}$, the change of orientation, is defined from Eqs. (10) and (11) as

$$\Delta\boldsymbol{\alpha} = vect(\Delta\boldsymbol{Q}\boldsymbol{Q}^{T}) \tag{32}$$

where $\Delta\mathbf{Q}$ is the variation of the rotation matrix and vect(.) is the vector linear invariant of its matrix argument.
Similarly, Eq. (20) can also be written, for small displacements, as

$$\mathbf{J}_{\text{passive}}^{\text{T}}\Delta\boldsymbol{\theta}_{\text{passive}} \cong \Delta\mathbf{c} \tag{33}$$

where $\Delta\boldsymbol{\theta}_{\text{passive}}$ is a vector of small variations of the joint coordinates of the constraining leg. Substituting Eq. (29) into Eq. (30), one obtains

$$\mathbf{B}^{-1}\mathbf{A}\Delta\mathbf{c} = \mathbf{C}\mathbf{B}^{\text{T}}(\mathbf{A}\mathbf{J}_{\text{passive}})^{-\text{T}}\mathbf{J}_{\text{passive}}^{\text{T}}\mathbf{w} \tag{34}$$

Premultiplying both sides of Eq. (34) by B, and substituting Eq. (33) into Eq. (34), one obtains,

$$\mathbf{AJ}_{\text{passive}}\Delta\boldsymbol{\theta}_{\text{passive}} = \mathbf{BCB}^{\text{T}}(\mathbf{AJ}_{\text{passive}})^{-\text{T}}\mathbf{J}^{\text{T}}_{\text{passive}}\mathbf{w} \tag{35}$$

Then, pre-multiplying both sides of Eq. (35) by $(\mathbf{AJ}_{\text{passive}})^{-1}$, one obtains,

$$\Delta\boldsymbol{\theta}_{\text{passive}} = (\mathbf{AJ}_{\text{passive}})^{-1}\mathbf{BCB}^{\text{T}}(\mathbf{AJ}_{\text{passive}})^{-\text{T}}\mathbf{J}^{\text{T}}_{\text{passive}}\mathbf{w} \tag{36}$$

and finally, premultiplying both sides of Eq. (36) by $\mathbf{J}_{\text{passive}}$, one obtains,

$$\Delta\mathbf{c} = \mathbf{J}_{\text{passive}}(\mathbf{AJ}_{\text{passive}})^{-1}\mathbf{BCB}^{\text{T}}(\mathbf{AJ}_{\text{passive}})^{-\text{T}}\mathbf{J}^{\text{T}}_{\text{passive}}\mathbf{w} \tag{37}$$

Hence, one obtains the Cartesian compliance matrix as

$$\mathbf{C_c} = \mathbf{J}_{\text{passive}}(\mathbf{AJ}_{\text{passive}})^{-1}\mathbf{BCB}^{\text{T}}(\mathbf{AJ}_{\text{passive}})^{-\text{T}}\mathbf{J}^{\text{T}}_{\text{passive}} \tag{38}$$

with

$$\Delta\mathbf{c} = \mathbf{C}_{\mathbf{c}}\mathbf{w} \tag{39}$$

where $\mathbf{C}_c$ is a symmetric positive semi-definite (6×6) matrix, as expected.
It is noted that, in non-singular configurations, the rank of B, C and $\mathbf{J}_{\text{passive}}$ is five, and hence the rank of $\mathbf{C}_c$ will be five, depending on the degree of freedom of the mechanism. Hence, the nullspace of matrix $\mathbf{C}_c$ will not be empty and there will exist a set of vectors w that will induce no Cartesian displacement $\Delta\mathbf{C}$. This corresponds to the wrenches that are supported by the constraining leg, which is considered infinitely rigid. These wrenches are orthogonal complements of the allowable twists at the platform. Hence, matrix $\mathbf{C}_c$ cannot be inverted and this is why it was more convenient to use compliance matrices rather than stiffness matrices in the above derivation.
Furthermore, the diagonal elements of the stiffness matrix are used as the system stiffness value. These elements represent the pure stiffness in each direction, and they reflect the rigidity of machine tools more clearly and directly. The objective function for mean value and standard deviation of system stiffness can be written as:

$$\boldsymbol{\mu}\text{-compliance} = \text{E}(\text{tr}(\mathbf{C}_{\text{c}})) \tag{40}$$

$$\boldsymbol{\sigma}\text{-compliance} = \text{STD}(\text{tr}(\mathbf{C}_{\text{c}})) \tag{41}$$

Where E(.) and STD(.) represent the mean value and the standard deviation respectively, and *tr* is the trace of the stiffness matrix.

4. Design optimization

4.1 Principles

We propose the mean value and the standard deviation of the trace of the generalized compliance matrix as the design indices. The purpose of design optimization is to evolve the performance indices by adjusting the structure parameters. It is noted that the trace of the matrix is an invariant of the matrix, so the distribution of the system stiffness/compliance is the distribution of the trace. The mean value represents the average compliance of the parallel robot manipulator over the workspace, while the standard deviation indicates the compliance fluctuation relative to the mean value. In general the lower the mean value the

less the deformation. Similarly, the lower the standard deviation the more uniform the stiffness distribution over the workspace. The suitability of these design indices for the system stiffness can be examined by developing their relationship with the stiffness of links and joints. We will further study a design optimization based on the compliance indices.

Since only a few geometric parameters can be handled due to the lack of convergence, this arises from the fact that traditional optimization methods use a local search by a convergent stepwise procedure, e.g. gradient, Hessians, linearity, and continuity, which compares the values of the next points and moves to the relative optimal points (Gosselin & Guillot, 1991). Global optima can be found only if the problem possesses certain convexity properties which essentially guarantee that any local optima are a global optimum. In other words, conventional methods are based on a point-to-point rule; it has the danger of falling in local optima. The genetic algorithms are based on the population-to-population rule; it can escape from local optima.

Genetic algorithms have the advantages of robustness and good convergence properties:

- They require no knowledge or gradient information about the optimization problems; only the objective function and corresponding fitness levels influence the directions of search.
- Discontinuities present on the optimization problems have little effect on the overall optimization performance.
- They are generally more straightforward to introduce, since no restrictions for the definition of the objective function exist.
- They use probabilistic transition rules, not deterministic ones.
- They perform well for large-scale optimization problems.

4.2 Optimization

In order to obtain the maximum global stiffness, the global compliance (since there are infinite terms among the diagonal stiffness elements) is minimized. As Cartesian stiffness is a monotonically increasing function of the link and actuator stiffness, the optimum solution always corresponds to the maximum link or actuator stiffness and these parameters are not included in the optimization variables. Seven geometrical parameters are selected as the pending optimization variables in order to obtain the optimal system stiffness, i.e.

$$\mathbf{s} = [\mathrm{R_p}, \mathrm{R_b}, \mathrm{l_{61}}, \mathrm{l_{62}}, \mathrm{z}, \mathrm{T_p}, \mathrm{T_b}] \tag{42}$$

where R_p is the radius of the platform, R_b is the radius of the base, l_{61}, l_{62} are the link length for the 1st and 2nd link of the passive leg, respectively,z is the height of the platform, T_p,T_b are the angles to determine the attachment points on the base and on the platform, and their bounds are

$$\begin{aligned}
&R_p \in [0.10, 0.14]m,\ R_b \in [0.20, 0.26]m,\\
&l_{61} \in [0.52, 0.70]m, l_{62} \in [0.52, 0.70]m,\\
&z \in [0.66, 0.70]m,\\
&T_p \in [18, 26]^\circ, T_b \in [38, 48]^\circ
\end{aligned}$$

Some genetic parameters and operators are set as:
Variable representation format: real value
Selection: roulette wheel approach

Crossover operator: multi-point crossover
Crossover rate: 0.9
Mutation operator: multiple-point bit mutation
Mutation rate: 0.005
Population size: 200
Maximum number of generations: 40
The input vectors are the random arrangement of discretization values from the seven structure variables. The objective function is defined as

$$ObjFun = E(tr(\mathbf{C}_c)) + STD(tr(\mathbf{C}_c)) = \mu + \sigma \tag{43}$$

The evolution of system stiffness/compliance value arises from the optimization of architecture and behaviour variables in the implementation process of genetic algorithm as shown in Figure 4. By simultaneously adjusting the seven parameters, optimization results are obtained after 40 generations as follows

$$\mathbf{s} = [R_p, R_b, l_{61}, l_{62}, z, T_p, T_b]$$

$$= [0.14m, 0.209m, 0.52m, 0.7m, 0.66m, 18^\circ, 48^\circ]$$

and the compliances in each direction are

$$\mathbf{K} = \left[\mathcal{K}_{\theta x}, \mathcal{K}_{\theta y}, \mathcal{K}_{\theta z}, \mathcal{K}_x, \mathcal{K}_y, \mathcal{K}_z \right]$$

$$= \left[0.0363, 0.0293, 0.0381, 0.0413, 0.0177, 0.0002 \right]$$

Figure 5 describes the evolution of the best individual, and the sum of the compliances is convergent at 0.0691 m/N after 40 generations.

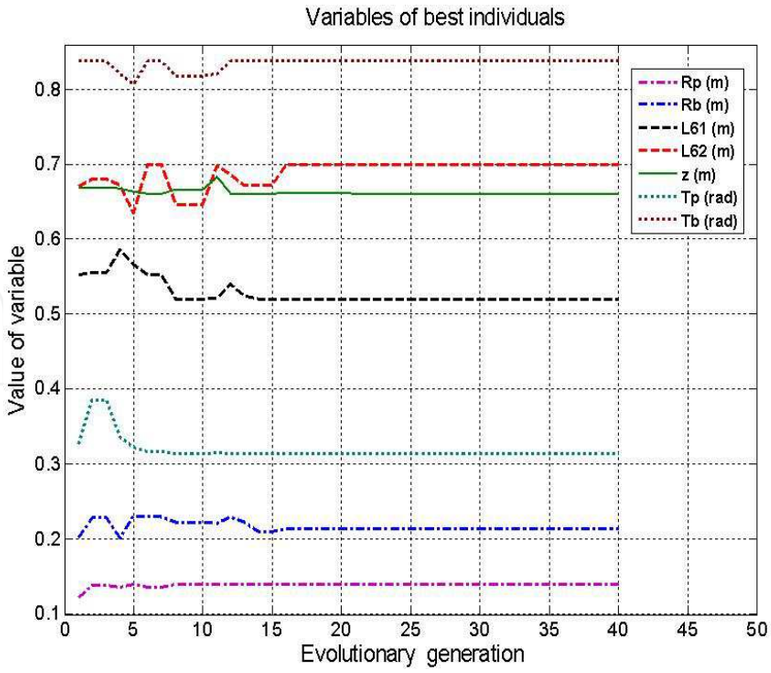

Fig. 4. The evolution of geometrical parameters for stiffness index

Before optimization, the parameter values of the mechanism were given as

$$\begin{aligned}\mathbf{s}' &= [R_p, R_b, l_{61}, l_{62}, z, T_p, T_b] \\ &= [0.11m, 0.25m, 0.68m, 0.52m, 0.68m, 22^\circ, 42^\circ]\end{aligned}$$

and the compliances in each direction were

$$\begin{aligned}\mathbf{K} &= \left[K'_{\theta x}, K'_{\theta y}, K'_{\theta z}, K'_x, K'_y, K'_z \right] \\ &= [0.1224, 0.1971, 0.7151, 0.0640, 0.0198, 0.0003]\end{aligned}$$

the compliance sum is 0.6416 m/N. After optimization, the compliance sum is improved 9.3 times.

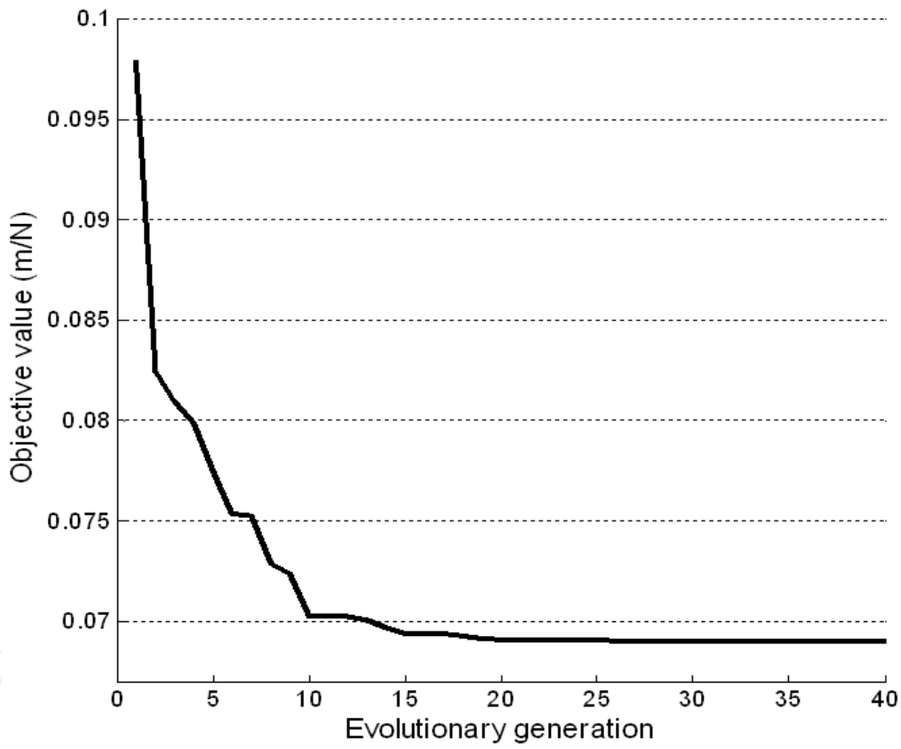

Fig. 5. The evolution of the performance

5. Conclusions

This chapter focused on the stiffness optimization of a spatial 5-DOF parallel manipulator. It is shown that the mean value and the standard deviation of the trace of the generalized compliance matrix can not only be used to characterize the kinetostatic behaviour of PKMs globally, but can be used for design optimization. This methodology paves the way for providing not only the effective guidance, but also a new approach of dimensional synthesis for the optimal design of general parallel mechanisms.

6. References

Zhang D, Gosselin C M. Kinetostatic modeling of parallel mechanisms with a passive constraining leg and revolute actuators. Mech Mach Theory, 2000, 37: 599-617

Dunlop G R, Jones T P. Position analysis of a two DOF parallel mechanism-Canterbury tracker. Mech Mach Theory, 1999, 34: 599-614

Carretero J A., Podhorodeski R P, Nahon M N, *et al*. Kinematic analysis and optimization of a new three degree-of-freedom spatial parallel manipulator. J Mech Design, 2000, 122:17-24

Staicu S, Zhang D, Rugescu R D. Dynamic modelling of a 3-DOF parallel manipulator using iterative matrix relations. Robotica, 2006, 24(1):125-130

Zhang D, Wang L. PKM capabilities and applications exploration in a collaborative virtual environment. Robot Cim-Int Manuf, 2000, 22: 384-395

Liu X J, Wang J S, Pritschow G. A new family of spatial 3-DoF fully-parallel manipulators with high rotational capability. Mech Mach Theory, 2005, 40: 475-494

Bi Z M, Lang S Y, Zhang D, *et al*, An integrated design toolbox for tripod-based parallel kinematic machines. J Mech Design, 2007, 129: 799-807

Birglen L, Gosselin C M. Kinetostatic analysis of underactuated fingers. IEEE T Robot, 2004, 20 (2):211 – 221

Chablat D, Angeles J. On the kinetostatic optimization of revolute-coupled planar manipulators. Mech Mach Theory, 2002, 37: 351-374

Zhang D and Gosselin C M. Parallel kinematic machine design with kinetostatic model. Robotica, 2002, 4(7): 429-438

Bergamaschi P R, Nogueira A C, Saramago S F. Design and optimization of 3R manipulators using the workspace features. Appl Math Comput, 2006, 172: 439-463

Stock M, Miller K. Optimal kinematic design of spatial parallel manipulators: Application to linear delta robot. J Mech Design, 2003, 125: 292-301

Rout B K, Mittal R K. Parametric design optimization of 2-DOF R–R planar manipulator: A design of experiment approach. Robot Cim-Int Manuf, 2008, 24:239-248

Ceccarelli M, Lanni C. A multi-objective optimum design of general 3R manipulators for prescribed workspace limits. Mech Mach Theory, 2004, 39:119-132

Mitchell J. H. Lum, Jacob Rosen, Mika N. Sinanan, et al. Optimization of a spherical mechanism for a minimally invasive surgical robot: theoretical and experimental approaches, IEEE T Bio-Med Eng, 2006, 53(7):1440 – 445

Zhao J S, Zhang S L, Dong J X. Optimizing the kinematic chains for a spatial parallel manipulator via searching the desired dexterous workspace. Robot Cim-Int Manuf, 2007, 23: 38-46

Boeij J, Lomonova E A, André J A, et al, Optimization of contactless planar actuator with manipulator, IEEE T Magn, 2008, 44(6):1118 -1121

Holland J. Adaptation in natural and artificial systems. The University of Michigan Press, Ann Arbor, MI, 1975

Gosselin CM, Guillot M. The synthesis of manipulators with prescribed workspace, ASME J Mech Des 1991; 113(1):451-5.

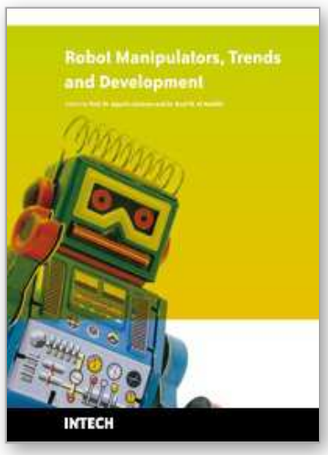

Robot Manipulators Trends and Development

Edited by Agustin Jimenez and Basil M Al Hadithi

ISBN 978-953-307-073-5
Hard cover, 666 pages
Publisher InTech
Published online 01, March, 2010
Published in print edition March, 2010

This book presents the most recent research advances in robot manipulators. It offers a complete survey to the kinematic and dynamic modelling, simulation, computer vision, software engineering, optimization and design of control algorithms applied for robotic systems. It is devoted for a large scale of applications, such as manufacturing, manipulation, medicine and automation. Several control methods are included such as optimal, adaptive, robust, force, fuzzy and neural network control strategies. The trajectory planning is discussed in details for point-to-point and path motions control. The results in obtained in this book are expected to be of great interest for researchers, engineers, scientists and students, in engineering studies and industrial sectors related to robot modelling, design, control, and application. The book also details theoretical, mathematical and practical requirements for mathematicians and control engineers. It surveys recent techniques in modelling, computer simulation and implementation of advanced and intelligent controllers.

INTECH
open science | open minds

InTech Europe
University Campus STeP Ri
Slavka Krautzeka 83/A
51000 Rijeka, Croatia
Phone: +385 (51) 770 447
Fax: +385 (51) 686 166
www.intechopen.com

InTech China
Unit 405, Office Block, Hotel Equatorial Shanghai
No.65, Yan An Road (West), Shanghai, 200040, China
中国上海市延安西路65号上海国际贵都大饭店办公楼405单元
Phone: +86-21-62489820
Fax: +86-21-62489821

IntechOpen